A Novel Setting-Free Parameter-Based Approach for Loss of Excitation Protection in Synchronous Generators

Mehdi Samami[1], Milad Niaz Azari[2*]

***Abstract*-- Loss of excitation (LOE) phenomenon can be hazardous for both the generator and power network stability. Previously presented LOE protection techniques are usually on the basis of the generator terminal impedance trajectory which have various drawbacks. Therefore, this study proposes a fast and reliable setting-free LOE detection method. For this aim the derivative of various parameters of the generator including resistance (R), reactance (X), reactive power (Q) and flux (φ) have been utilized in order to propose three different combined indices. Consequently the performance of the proposed protection algorithm has been evaluated by simulations, considering all the introduced indices in order to select the best one. The simulations have been carried out in MATLAB software, under different operating scenarios. The extracted results demonstrate the best performance of the last combined index, which is based on using the derivative of R, Q and φ. This index also shows amazing speed, accuracy, and reliability in detection of LOE and discrimination of LOE with stable power swing (SPS), compared with the conventional impedance-based methods.**

***Index Terms*-- Synchronous generator, loss of excitation, stable power swing.**

I. INTRODUCTION

A. Motivation and problem description

LOSS of excitation (LOE) fault is considered an important and usual fault in synchronous generators, which can stem from different factors such as unexpected opening of the excitation system switch, occurrence of fault in the excitation circuit, failure of the auxiliary components of the excitation system, etc. [1, 2]. This fault can be harmful for both the generator and power system. By interruption of the generator excitation system, it performs the same as an induction generator, absorbing a huge amount of reactive power from the power network. In fact, the machine tries to compensate the air-gap flux from the reactive power of the network. This issue can lead to over temperature in the body of the rotor and also the stator end core winding. Besides, LOE can also threaten the voltage stability in the power system and cause a subsequent black out in case of unstable power swings or out of step conditions, imposing on the generator [3-5].

B. Related works

Over the years, several approaches have been presented to develop the generator LOE and the other fault protection [6-32]. Under current relays are considered the earliest LOE protectors [6]. But the mentioned relays are not reliable for LOE detection because they cannot discriminate between an intentional decrement of the excitation current during light capacitive loading and an actual LOE. The second generation of LOE relays concentrated on various impedance-based methods such as the Mason single off-set zone relay [7], the Tremaine impedance-based relay [8], and the Berdy relay with two offset Mho characteristics [9]. Investigation [10] detects the LOE by measuring the admittance instead of impedance. In fact, impedance-based schemes are widely used for LOE detection. But various mal-operations of such relays have been reported repeatedly during stable power swing (SPS) and under light capacitive loading of the generator. Berdy relays usually utilize intentional time delay to avoid mal-operation during SPS conditions which can be hazardous in the case of an actual LOE. In recent years, in order to develop the speed and accuracy of the earlier LOE relays, some new schemes have been suggested. A support vector machine (SVM) [13–17], fuzzy inference [12], and artificial neural networks [11] are a few of the artificial intelligence approaches that underpin some of the schemes that have been presented. Large amounts of training data and potent processors are needed for these approaches' intricate computations, which is seen as one of their main disadvantages. In references [18, 19] LOE is detected, based on multiplication of voltage ($\boldsymbol{V}$), load angle ($\boldsymbol{\delta}$) and reactive power ($\boldsymbol{Q}$) variations. $\boldsymbol{\delta}$ has been approximated by these investigations, since measurement of $\boldsymbol{\delta}$ is a difficult task. So, the accuracy of this method is not as desired. Another contribution [20] detects LOE by utilizing the variation of the generator resistance. But this method does not demonstrate desirable behavior because of the reset of the relay in high slip frequency due to the oscillation of resistance in the case of LOE. Reference [21] presents an adaptive impedance-based scheme to remove the influence of static synchronous compensator (STATCOM) on the performance of LOE relay by means of Thevenin's model parameters at the STATCOM location. STATCOM is a fast-acting device capable of providing or absorbing reactive current and thereby regulating the voltage at the point of connection to a power grid. It is categorized under flexible AC transmission system (FACTS) devices. In this method, transmission of the LOE relay location is done by communication channel. So, in case of failure in the

1. Mehdi Samami, Department of electrical engineering, Sari branch, Islamic Azad University, Sari, Iran.
2. Department of electrical engineering, University of Science and Technology of Mazandaran, Behshahr, Iran.
Corresponding author Email: miladniazazari@mazust.ac.ir

communication system, this technique may not show accurate and suitable performance. Another algorithm [22] detects LOE on the basis of digital phase comparison in the time domain. This method is a slow detection method that cannot discriminate SPS. Another approach [23] detects LOE on the basis of an estimation of field current and comparing it with the measured one. In the case of an LOE, the difference between these two values is impressive. Another technique [24] protects the generator against LOE by utilizing a new index consisting of the first and second derivatives of reactive power, which finally reduces the relay operation time in comparison with the impedance-based relays. However, the reduced operation time is not significant. Internal voltage of the generator can also be a significant parameter for LOE detection [25, 26]. In ref. [26], a combined index of multiplying the internal voltage and reactive power is used to highlight the decreasing changes and also the negative polarity of variations during LOE. This technique improved the operation time of the relay but not as desired. Investigation [27] proposed a new LOE detection method on the basis of increasing the reactive power strategy and monitoring the output voltage of the generator terminal. Because of this, while the generator voltage is under LOE conditions, it does not experience incremental fluctuations due to a decrease in the filed current, but when it is under non-LOE conditions, it may exhibit growing behavior. During LOE, the aforementioned method's speed is undetectable. Moreover, there is some unreliability in this approach during SPS. Another method for detecting LOE is to use the load angle off the generator [28]. Because the load angle of the parallel generators shows diminishing variations during LOE, whereas the load angle of the excitation interrupted generator grows. The challenge of measuring the load angle is the method's downside. References [29, 30] examine how SVC and STATCOM affect conventional impedance-based relay performance, respectively. Accordingly, the presence of fact devices imposes additional time delay on the relay and increases the risk of an out-of-step condition or changes the stable operating point of the generator without losing the synchronism. Two methods are introduced in [29] to decrease the delay caused by STATCOM for the LOE relay operation time by applying the phase domain model and also the d-q model of the generator. In both models, the reduction of time delays is good but not satisfying. On the other hand, in accordance with [30], it is concluded that the positive offset type of LOE relay can detect and eliminate the SVC effect faster than other traditional impedance-based relays. Ref [31] proposed a method based on generator voltage and current signals waveforms envelopes analysis. Separating LOE from SPS is the focus of different research [32], which applies a transient model of a synchronous generator based on frequency decomposition and time domain analysis of three crucial parameters: voltage, active, and reactive powers. But in terms of differentiating LOE from SPS, this approach enhanced the relay's accuracy and dependability. However, the projected improvement in operation speed was not realized. Stated differently, the focus of this work is not on relay speed but rather on improving relay security and accuracy.

C. Contribution

This contribution presents a novel algorithm on the basis of three different new combined indices, using the derivative of some generator key parameters such as resistance (R), reactance (X), reactive power (Q) and flux (φ).

The main drawbacks of various presented LOE schemes [6-32], include:

1) Low and undesired speed of operation
2) Low reliability and accuracy in diagnosing SPS

So, diligent efforts to present suitable methods to decrease the time of operation and increase the security and reliability of the relay in various potential scenarios were made in recent years. Accordingly, this study tried to present a new technique using accessible parameters of the generator, considering various loadings of the generator following both total and partial LOE, with the following advantages.

1) The speed of operation of the proposed technique is improved in comparison with too many of the newly presented methods, which leads to decreasing the risk of damage to the generator and power network.
2) The proposed indices demonstrated great ability to distinguish LOE from SPS and other disturbances (increment of accuracy and reliability of the proposed relay).

II. CONVENTIONAL SCHEME OF LOE PROTECTION

As stated earlier, the impedance-based method with concentration on Berdy scheme is the most usual method of LOE protection. The characteristic of the conventional relay is consist of two circular protective zones as follows: [1, 5].

- First zone, for heavy load condition, time delay: 0.1 s.
- Second zone, for light load condition, time delay: about 0.6 s.

In order to prevent mal-operation of the relay during SPS, the second zone is equipped with an approximate intentional time delay of 0.6 s. This time delay is considered the most important drawback of the Berdy relay. Because it causes a delay in the case of an actual LOE, which is not desired and can be hazardous for both the generator and power system.

Fig. 1. illustrates the protective characteristics of the conventional relay. Accordingly, the diameter of the smaller zone is set to 1 per unit, and the diameter of the bigger zone is set to the generator synchronous reactance (x_d). The characteristics have an offset, which is equal to half of the transient reactance ($x'_d/2$). As shown in Fig. 1, the rate of variation in impedance trajectory is faster in heavy loads compared with light loads. On the other hand, the impedance trajectory can enter the protective zone and exit from it in the case of SPS, which can lead to the relay mal-operation.

III. PROPOSED LOE PROTECTION TECHNIQUE

A. Introduction of the utilized parameters

As previously mentioned, this study tries to present a reliable and fast LOE detection technique on the basis of the generator parameters. So, in the first step, the mentioned parameters, which are obviously influenced following an LOE, should be measured or calculated. Impedance components including $\boldsymbol{R}$ and $\boldsymbol{X}$ are considered as initial parameters which are utilized in the first index of this paper. In order to calculate $\boldsymbol{R}$ and $\boldsymbol{X}$,

assume a generator that is connected to the external grid via a power transformer. The equivalent circuit of the mentioned network is illustrated in Fig. 2. Accordingly, $\boldsymbol{E_G}$ and $\boldsymbol{E_{Syst}}$ are the magnitude of the generator internal voltage and the power system equivalent voltage respectively. Besides, $\boldsymbol{X_T}$ and $\boldsymbol{X_{Syst}}$ represent the reactance of the transformer and power system respectively. It is noteworthy that, $\boldsymbol{X_G(t)}$ is the reactance of the generator during LOE. After the LOE event, $\boldsymbol{X_G(t)}$ changes until it settles to a final value between $\boldsymbol{(x_d'' + x_q'')/2}$ and $\boldsymbol{(x_d + x_q)/2}$, as derived in (1), where $\boldsymbol{x_d''}$ and $\boldsymbol{x_q''}$ are the sub-transient reactance of the direct and quadrature axis of the generator. On the other side, $\boldsymbol{x_d}$ and $\boldsymbol{x_q}$ represent the direct and quadrature axis synchronous reactances.

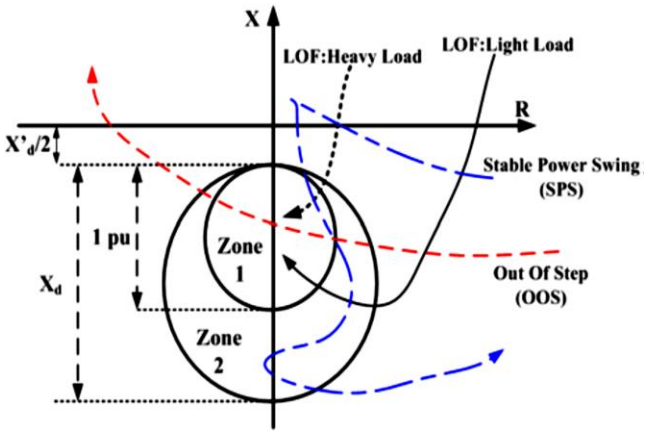

Fig 1. Conventional LOE relay protection zones and the impedance trajectory in various conditions [19]

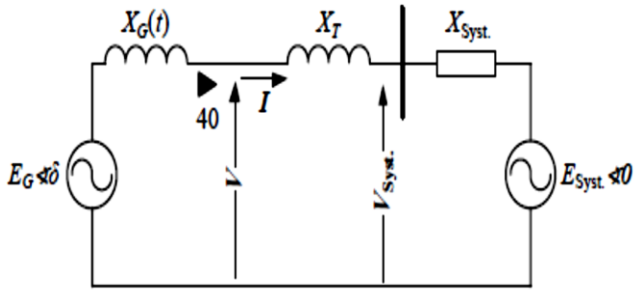

Fig. 2. Equivalent circuit of a generator, connected to power system via a transformer [20]

$$(x_d'' + x_q'')/2 < X_G(t) < (x_d + x_q)/2 \quad (1)$$

The following equations can be derived, considering Fig. 2, [20].

$$V = E_G\angle\delta - jX_G(t).I \quad (2)$$

$$I = \frac{E_G\angle\delta - E_{Syst}\angle 0}{j(X_G(t) + X_T + X_{Syst})} \quad (3)$$

By dividing voltage to current and assuming $k = E_{Syst}/E_G$, the impedance, seen by the generator terminal can be calculated as follows [20].

$$Z = \frac{V}{I} = \frac{E_G\angle\delta - jX_G(t).I}{I} = \frac{E_G\angle\delta}{I} - jX_G(t) \quad (4)$$

$$Z = \frac{V}{I} = \frac{K\sin\delta}{1+K^2-2K\cos\delta}\cdot X_{Tot}(t) + j.\left(\frac{1-k\cos\delta}{1+k^2-2k\cos\delta}\cdot X_{Tot}(t) - X_G(t)\right) \quad (5a)$$

$$X_{Tot}(t) = X_G(t) + X_T + X_{syst} \quad (5b)$$

The resistance and reactance of the generator can be extracted from (1) as below.

$$Real\ (Z) = R(t) = \frac{K(t)\cdot\sin\delta}{1 + K(t)^2 - 2k\cos\delta}\cdot X_{Tot}(t) \quad (6)$$

$$Img\ (Z) = X(t) = \frac{1-K(t)\cos\delta}{1+K(t)^2-2K(t)\cos\delta}\cdot X_{Tot}(t) - X_G(t) \quad (7)$$

The second utilized parameter for LOE detection is reactive power (Q). This parameter is calculated by (4). where V_T and X_d' are the generator terminal voltage and transient reactance respectively [33]. It is noteworthy that, the reactive power can also be obtained, using three phase voltages and currents as mentioned in (9).

$$Q = V_T\left(\frac{E_G}{X_d'}cos\delta - \frac{V_T}{X_d'}\right) \quad (8)$$

$$Q = image(V_1 \times I_1^* + V_2 \times I_2^* + V_3 \times I_3^*) \quad (9)$$

The last parameter of this study for LOE detection is flux ($\boldsymbol{\varphi}$). In this paper, two different methods are introduced in order to achieve the magnetic flux of the generator. The first way to measure the magnetic flux is using search coils, which are located through the slots of the stator of the generator [34-37]. Fig. 3 shows a schematic representation of the search coil sensor that locates along the stator teeth. The search coil sensor's theory is based on Faraday's law of induction. As a result, the voltage produced in a single turn of a sample generator's search coil sensor may be found as indicated in (10), [36-37].

$$e_{ind} = (v \times B).L \quad (10)$$

where $\boldsymbol{v}$, $\boldsymbol{B}$ and $\boldsymbol{L}$ represent the component of the wire velocity which is perpendicular to the direction of flux density, the magnetic flux of the generator and the measured length of the search coil sensor, respectively.

By altering the air gap flux in a coiled conductor, a voltage is generated between the coil leads. The induced voltage mainly depends on the rate of flux variation. The flux will change through the coil by locating the coil in a time variant-magnetic field. The search coils can obviously sense the flux density distribution of the air gap. The signal detected by a search-coil sensor depends on different items, i.e., the permeability of the area that the coil is located in, the material of the core, the number of turns, and ultimately, the rate of flux variation through the coil. It is worth noting that, since this sensor is easily accessible and its cost is really reasonable, a high number of it can be applied in the slots of the generator stator for an increment of accuracy in the proposed relay performance.

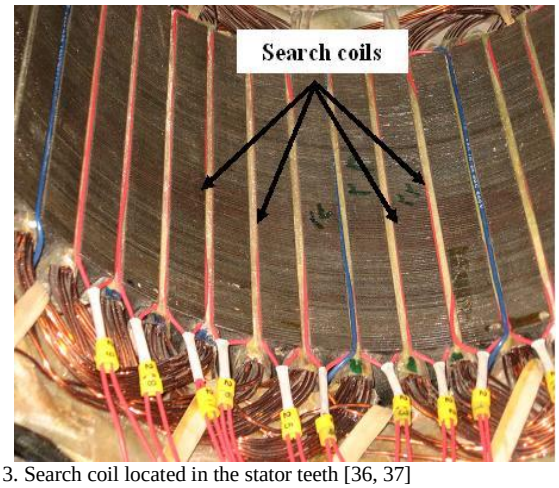

Fig. 3. Search coil located in the stator teeth [36, 37]

But using search coils in the slots of the generator is not possible in some cases. So, a more common method which is applicable for all cases should be introduced. Therefore, this paper proposes a reliable technique to estimate the amount of magnetic flux for LOE detection. This method is based on calculation of the flux by means of related mathematical equations and implementation of the final equation of flux variations by a computerized simulation.

Accordingly, the flux equation is extracted from the voltage equation of the generator as follows [38].

$$v = \frac{-d\lambda}{dt} \tag{11}$$

where λ is equal to multiplication of flux by the number of stator coil turns.
On the other side, λ can be calculated as below [38].

$$\lambda = k_w N_{ph} \varphi_p \cos(\omega_e t) \quad , \quad \omega_e = \left(\frac{poles}{2}\right)\omega_m \tag{12}$$

where k_w, N_{ph} and φ_p represent coil or winding factor, the number of turns of the stator coil and the magnetic flux per pole, respectively. Furthermore, ω_e is the electrical angular velocity and ω_m is the mechanical angular velocity.

Finally, by integrating equation (12), the amount of flux variation is obtained as follows.

$$\varphi_p = \frac{-1}{k_w N_{ph} \cos(\omega_e t)} \int v \, . \, dt \tag{13}$$

The amount of estimated flux is really close to the measured flux by the search coils. On the other hand, all variables of the generator, extracted from the magnetic flux, are proportional to the measured ones from the search coil sensors [38]. So, the flux, obtained from this method can be used for LOE detection method with high accuracy and reliability.

B. Developing the idea

This investigation introduces three different combined LOE indices (LOEI). Each index consist of multiplication of two or three terms, and each term shows the rate of variations of the aforementioned generator parameters over time (time derivative of the parameters), following an LOE.

The first index is known as derivative of impedance LOE index (DILOEI) and can be written as follows.

$$DILOEI = \frac{dR}{dt} \cdot \frac{dX}{dt} \tag{14}$$

In case of an LOE, DILOEI should be positive. Because the derivative of R and X are both negative following an LOE. In order to prove this theory the derivative of R and X should be calculated, considering (6) and (7), as follows.

$$\frac{dR}{dt} = \frac{(1-K(t)^2)\cdot sin\,\delta}{(1+K(t)^2-2K(t)\,cos\,\delta)^2} \cdot \frac{dK}{dt} \cdot X_{Tot}(t) + \frac{K(t)\cdot sin\,\delta}{1+K(t)^2-2K(t)\,cos\,\delta} \cdot \frac{dX_{Tot}(t)}{dt} \tag{15}$$

$$\frac{dX}{dt} = \frac{(1+K(t)^2)\cdot cos\,\delta-2k(t)}{(1+K(t)^2-2K(t)\,cos\,\delta)^2} \cdot \frac{dK}{dt} \cdot X_{Tot}(t) + \frac{1-k(t)\,cos\,\delta}{1+K(t)^2-2K(t)\,cos\,\delta} \cdot \frac{dX_{Tot}(t)}{dt} \tag{16}$$

In case of an LOE and before losing of synchronism, in accordance to (15) and (16), $\boldsymbol{K}$ starts increasing while $\boldsymbol{\delta}$ is almost constant or shows small incremental behavior. Therefore $\boldsymbol{dK/dt}$ is positive. While $\boldsymbol{E_{syst} < E_G}$, the first term of (15) and (16) are positive and negative respectively. In this condition, no danger threatens the generator and power network. Because the flow of reactive power toward the generator is normal. It is noteworthy that, after a few seconds the second term of (15) and (16) will become zero. This issue is caused by settling of $\boldsymbol{X_G(t)}$ to its final value. At this moment the value of $\boldsymbol{K}$ increases to more than 1 and consequently $\boldsymbol{1-K(t)^2}$ in the first term of (15) becomes negative while $\boldsymbol{dK/dt}$ is still positive. Therefore, after a certain time, $\boldsymbol{dR/dt}$ becomes and remains negative. On the other hand, after an LOE, since $\boldsymbol{K > 1}$ and the value of $\boldsymbol{\delta}$ increases with a slow rate before out of step condition, therefore, in the first term of (13), $\boldsymbol{(1+K(t)^2)\cdot cos\,\delta < 2k(t)}$ while $\boldsymbol{dK/dt}$ is still positive. As a result, $\boldsymbol{dX/dt}$ will become and remain negative. It should be noticed that, in motoring and also in unstable mode of operation of a synchronous generator, $\boldsymbol{(1+K(t)^2)\cdot cos\,\delta}$ is negative. So, $\boldsymbol{dX/dt}$ will become and remain negative again.

The second LOE detection index is known as derivative of resistance and reactive power LOE detection index (DRPLOEI) and can be written as follows.

$$DRPLOEI = \frac{dR}{dt} \cdot \frac{dQ}{dt} \tag{17}$$

When an LOE occurs, DRPLOEI should be positive. Because the derivative of R and Q are both negative. The negative sign of dR/dt in such condition was stated earlier. But, in case of an LOE, the generator absorbs a huge amount of Q from the network [33]. So, the generator voltage and reactive power show an obvious decreasing behavior as illustrated in Fig. 3. This issue can also be confirmed by (4). Accordingly, after occurrence of LOE, the values of E_G and V_T decrease and on the other hand, by increment of δ, the value of $cos\delta$ decreases obviously. As a result, the value of Q shows decreasing behavior and consequently the derivative of Q will be negative.

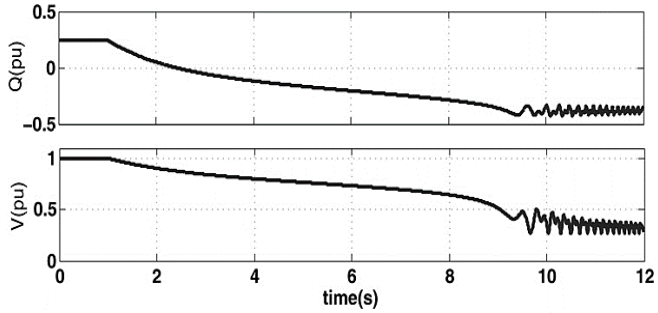

Fig. 4. Variation of voltage and reactive power following an LOE [33]

The third proposed LOE detection index is consist of three terms and is known as derivative of resistance, reactive power and flux LOE detection index (DRPFLOEI) which is presented as follows.

$$DRPFLOEI = \frac{dR}{dt} \cdot \frac{dQ}{dt} \cdot \frac{d\varphi}{dt} \quad (18)$$

In case of an LOE, DRPFLOEI should be negative. Because the derivative of $\boldsymbol{R}$, $\boldsymbol{Q}$ and $\boldsymbol{\varphi}$ are negative simultaneously. The negative sign of $\boldsymbol{dR/dt}$ and $\boldsymbol{dQ/dt}$ in LOE were proved earlier. After interruption of the excitation system, the magnetic air-gap flux starts decreasing seriously, as shown in Fig. 5, [36, 37]. The theory behind the high absorbing of reactive power by the generator stems from the significant reduction of the air-gap flux. So, the derivative of flux is also negative during LOE.

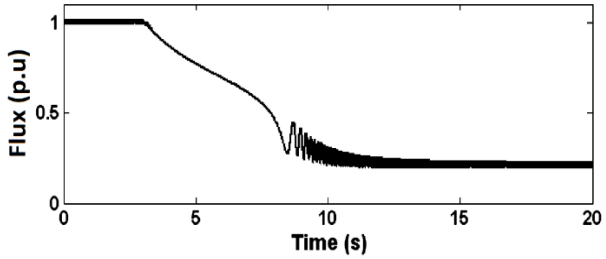

Fig. 5. Variation of flux following an LOE [36, 37]

C. Setting of Generator Steady-state Capability Limits

The under-excitation setting calculation is exactly the same as previous studies [39]. Fig. 6 depicts the steady-state capability limits for a synchronous generator. The under-excitation capability limits are expressed via two decisive parameters

- The stator current limit of the machine and also the steady-state stability limit (SSSL)
- Under-excitation limits (UEL)

SSSL shows how far a generator can work in leading power factor or under-excitation mode in the capability curve. On the other side, UEL is defined to avoid decrement of excitation over the stator end-region heating limits. The UEL is usually set to 80% to 85% SSSL or GUEC.

D. Discrimination of LOE with stable power swings

In previous section, three different LOE detection indices were proposed and it was proved that, DILOEI and DRPLOEI should be positive and DRPFLOEI must be negative following an LOE event. But, it is worth mentioning that, during a stable power swing (SPS) the same condition happens for all the introduced indices. So, discrimination of LOE from SPS is of prime importance. Since, $\boldsymbol{dR/dt}$ is the common term of all the proposed indices. Therefore, it plays an important role for this aim. In fact the maximum duration that $\boldsymbol{dR/dt}$ remains negative, following a power swing can be as a decisive factor for distinguishing LOE from SPS.

Under SPS condition, the values of $\boldsymbol{K}$, $\boldsymbol{X_G}$, $\boldsymbol{X'_d}$ and $\boldsymbol{X_{Tot}}$ can be assumed as constant values. It is noteworthy that, $\boldsymbol{X_G}$ and $\boldsymbol{X'_d}$ are very close to each other. So, in case of SPS, $\boldsymbol{dR/dt}$ can be written as follows.

$$\frac{dR}{dt} = \frac{dR}{d\delta} \cdot \frac{d\delta}{dt} = \frac{(1+K^2)\cdot K\cdot \cos\delta(t) - 2K^2}{(1+K^2-2K\cos\delta(t))^2} \cdot \frac{d\delta}{dt} \cdot X_{Tot} \quad (19)$$

According to Fig. 7, in normal condition the value of system voltage and the generator voltage are almost the same. Because the generator is paralleled to the external grid (system). Therefore, their voltages are unique. On the other hand, after occurrence of LOE or any similar disturbance, since the voltage of the generator starts decreasing, so the AVR tries to compensate the magnetic air-gap flux from the reactive power of the system. So, for flowing of reactive power from system toward the generator, the value of system voltage should be a little more than the voltage of the generator ($\boldsymbol{E_{syst} > E_G}$). Since both of the mentioned values are really close to each other. So, the ratio of $\boldsymbol{E_{Syst}/E_G}$ which is known as term K, becomes a little more than 1. The difference between $\boldsymbol{E_{Syst}}$ and $\boldsymbol{E_G}$ (range of variations of term K) is extremely small following LOE or SPS. So, term K can be considered 1. By assuming $\boldsymbol{K = 1}$, relation (19) can be summarized as below. It is noteworthy that, during SPS, $\boldsymbol{\delta}$ will change while the value of K is approximated to be constant (K=1).

$$\frac{dR}{dt} = \frac{2\cos\delta(t) - 2}{(1+K^2-2K\cos\delta(t))^2} \cdot \frac{d\delta}{dt} \cdot X_{Tot} \quad (20)$$

Since, $\boldsymbol{(2\cos\delta(t) - 2)}$ is always negative, so the sign of $\boldsymbol{dR/dt}$ and $\boldsymbol{d\delta/dt}$ are always opposite compared each other. As stated in [18-20], when a power swing occurs, $\boldsymbol{d\delta/dt}$ oscillates in the range of 0.3 to 7 Hz. Accordingly, the period of $\boldsymbol{d\delta/dt}$ is between 0.142 and 3.33s, as depicted in Fig. 8. So in the longest power swing, $\boldsymbol{d\delta/dt}$ remains positive for ½ of the period which is equal to 3.33/2 (1.67 s). Consequently, in the longest SPS, $\boldsymbol{dR/dt}$ does not remain negative for more than 1.67 s. Therefore, it can be concluded that, in LOE condition DILOEI and DRPLOEI should become and remain positive for more than 1.67 s and DRPFLOEI must become and remain negative for more than 1.67 s, otherwise the detected disturbance is a power swing.

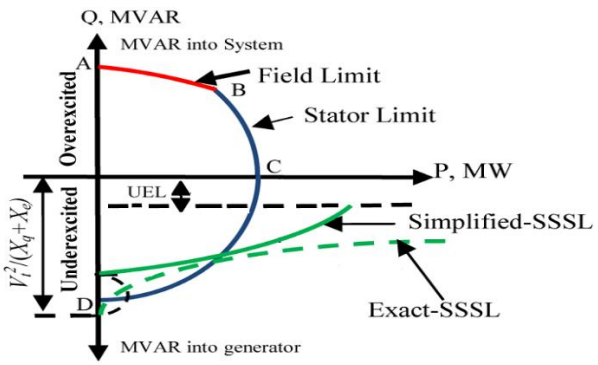

Fig. 6. Capability limits of the synchronous generator [39]

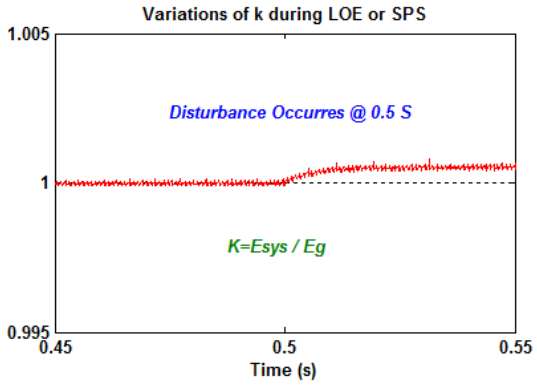

Fig. 7. Variation of K following LOE

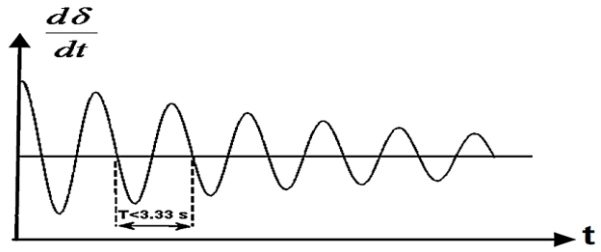

Fig. 8. Variation of $d\delta/dt$ following SPS [20]

E. Algorithm of the proposed technique

Fig. 9, depicts the algorithm of the proposed technique. Accordingly, the phasors of V and I are measured. The general structure of signal processing technique for calculation of R, X and Q is illustrated in Fig. 10. Accordingly, in the first step, the voltage and current are sampled by means of a sampling frequency. Then, by applying a quadrature oscillator, the signals are modulated by carrier signals. Low-pass filters are utilized for signal demodulation purposes. It is worth noting that, G_f is added in order to achieve a unity gain at the DC component. The outputs of low-pass filters are real and imaginary parts of the complex signal. So, the RMS values of the signal magnitude and phase can be obtained, using the following equations.

$$M = \frac{1}{\sqrt{2}}\sqrt{Re^2 + Im^2} \tag{21}$$

$$\theta = tan^{-1}\left(\frac{Im}{Re}\right) \tag{22}$$

The frequency deviation can also be written as follows.

$$\Delta Freq(n) = \frac{(6[\theta(n)-\theta(n-1)])+(3[\theta(n-1)-\theta(n-2)])+([\theta(n-2)-\theta(n-3)])}{20\pi/Fsampling} \tag{23}$$

where $\theta(n-m)$ is the phase angle output at the $(n-m)$ sample. Besides, n and $Fsampling$ represent the sample and the sampling frequency, respectively. Finally, this value can be utilized as a derivative filter. In order to compensate the magnitude error caused by frequency deviation, a compensation block for the P-Class filter is used. The magnitude compensation is done by the following equation.

$$\mathrm{M}_{Comp} = \frac{M}{Model_{filter-class}} \tag{24}$$

$Model_{filter-class}$ is known as the compensation factor of the filter and is calculated as below for P-Class filters.

$$Model_{P-Class} = sin\frac{\pi(f_0 + K_C\Delta Freq(i))}{2f_0} \tag{25}$$

where f_0 is the nominal frequency and K_C is obtained experimentally, which is equal to 1.625. Consequently R, X and Q are calculated using (1)-(9). But the flux is estimated by (11)-(13). It is noteworthy that, a second-order Butterworth low-pass filter with a cut-off frequency of 5 Hz is utilized in order to overcome the potential disturbances of the power network.

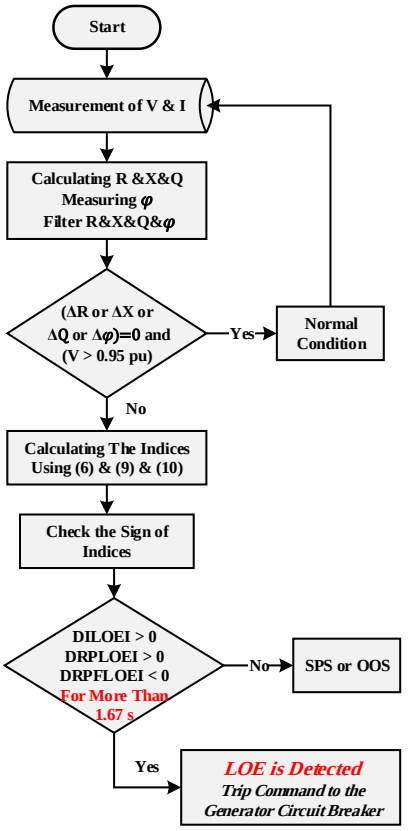

Fig. 9. Flowchart of the proposed method

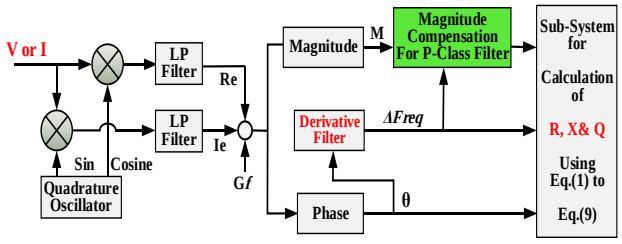

Fig. 10. Block diagram of calculating R, X and Q

If the mentioned filtered parameters show no variations and the value of voltage becomes more than 0.95 p.u, the normal condition is met. Otherwise, the decisive indices are calculated, utilizing (14), (17) and (18). If (14) or (17)

becomes and remains positive for more than 1.67 s, or (18) becomes and remains negative for more than 1.67 s, LOE is detected by the algorithm. Otherwise an SPS or OOS is occurred.

IV. SIMULATION AND EVALUATION OF THE PROPOSED STRATEGY

To evaluate the performance of the proposed algorithm and find the best LOE index, different simulation scenarios for all the presented indices have been carried out on a single machine infinite bus (SMIB) system and a three machine infinite bus (TMIB) system (see Fig. 11), considering various loading types and levels following different abnormal conditions. More details about the simulated system are presented in Appendix.

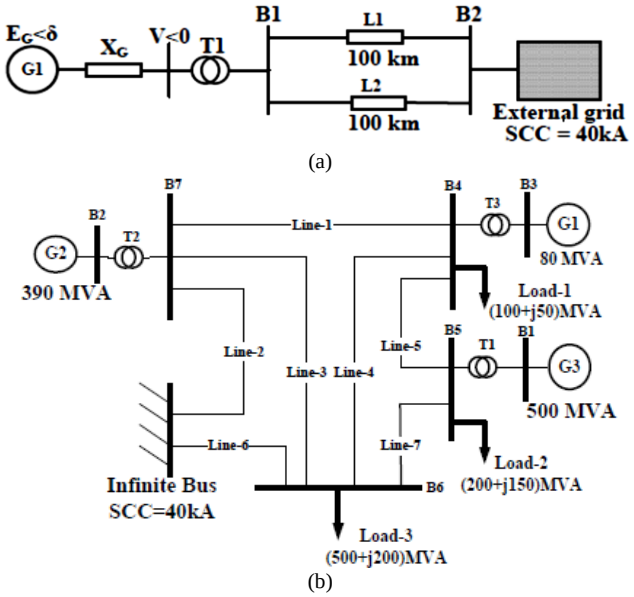

Fig. 11. Configuration of (a) SMIB system (b) TMIB system [23, 42]

A. Generator LOE

In this section, 8 different simulated scenarios are presented in Table I. Accordingly, the reaction of the introduced technique is studied on the sample SMIB network for both heavy and light inductive and also capacitive loading following Total LOE (TLOE) and Partial LOE (PLOE - 0.4 p.u.) conditions. In the studied network, a synchronous generator rated 390 MVA, 24 KV, is protected by the proposed LOE relay. Besides, the different loading conditions per unit utilized for this generator are illustrated in Table II.

TABLE I
Different Simulated Cases for LOE Detection of the Proposed Method

Loading Type	Case	Loading Value (p.u.)	Mode of LOE
Heavy loadings	1	L9=0.9+j0.3-lagging	TLOE, E_F=0
	2		PLOE, E_F=0.4
Light loadings	3	L2=0.1+j0.2-lagging	TLOE, E_F=0
	4		PLOE, E_F=0.4
Heavy loadings	5	L13=0.7-j0.5- leading	TLOE, E_F=0
	6		PLOE, E_F=0.4
Light loadings	7	L19=0.3-j0.2- leading	TLOE, E_F=0
	8		PLOE, E_F=0.4

Besides, the different loading points in per units utilized for this generator are illustrated in Table II.

TABLE II
Loading of Generator in Per Unit

S=(P+jQ) p.u.							
L1	0.1+j0.5	L6	0.5+j0.4	L11	0.9-j0.2	L16	0.5-j0.6
L2	0.1+j0.2	L7	0.7+j0.2	L12	0.7-j0.2	L17	0.3-j0.6
L3	0.3+j0.2	L8	0.7+j0.4	L13	0.7-j0.5	L18	0.3-j0.4
L4	0.3+j0.5	L9	0.9+j0.3	L14	0.5-j0.2	L19	0.3-j0.2
L5	0.5+j0.2	L10	0.9+j0.1	L15	0.5-j0.4	L20	0.1-j0.6

1) Total Loss of Excitation (TLOE)

This section studies the influence of TLOE on the performance of the different proposed indices. This condition might happen because of opening the circuit of the excitation system or opening the excitation switch. In cases 1, 3, 5 and 7 of Table 1, the excitation of the generator is completely interrupted ($E_F = 0$). Fig. 12a depicts the performance of DILOEI in heavy inductive loading of the network, following a TLOE at t=0 s (Case 1). On the other hand, Fig. 13a displays the behavior of DILOEI in heavy capacitive loading of the system, caused by a TLOE at t=0 s (Case 5). In such a condition, the voltage significantly decreases and the derivative of R and X becomes negative. As a result, DILOEI becomes and remains positive for more than 1.67 s. So, the relay issues the trip signal after 1.706 s for case 1 and 1.694 for case 5. In light inductive (case 3) and light capacitive (case 7) loading, the behavior of V, R and X are exactly the same as cases 1 and 5, and the trip signals are sent after 1.703 s and 1.698 s for cases 3 and 7, respectively.

Fig. 12b depicts the performance of DRPLOEI in heavy inductive loading of the network (case 1). On the other hand, Fig. 13b displays the behavior of DRPLOEI in heavy capacitive loading of the system, caused by a TLOE at t=0 s (Case 5). After a TLOE, the voltage decreases to less than 0.95 per unit and the derivative of R and Q becomes negative. Therefore, DRPLOEI becomes and remains positive for more than 1.67 s. Consequently, the relay issues the trip signal after 1.701 s for case 1 and 1.693 for case 5. For cases 3 and 7, the variations of V, R and Q are approximately the same in cases 1 and 5. So, the trip signals are issued after 1.700 s and 1.698 s for cases 3, 5, and 7, respectively.

Fig. 14a and 14b illustrate the performance of DRPFLOEI in heavy inductive (case 1) and heavy capacitive loading (case 5) following a TLOE. In both cases, the values of V, R , Q and φ show decreasing behavior and the derivative of R, Q and φ are negative. So, DRPFLOEI becomes and remains negative for more than 1.67 s. As a result, the LOE relay sends the trip command after 1.684 s and 1.679 s for case 1 and case 5, respectively. It is noteworthy that, the corresponding times are 1.684 s and 1.682 s for case 3 and 7 respectively.

Lastly, Table III provides an overview of the various suggested indexes' performance on the SMIB system under TLOE circumstances. In light of this, DRPFLOEI operates the fastest when compared to the other two indices. The time difference, though, is actually insignificant and should be disregarded. However, the suggested relay's behavior for every

index is essentially independent of the generator's loading.

TABLE III
Performance of Different Indices Following Tloe

Case	Loading Type	DILOEI	DRPLOEI	DRPFLOEI
1	L9=0.9+j0.3	1.706	1.701	1.684
3	L2=0.1+j0.2	1.703	1.700	1.684
5	L13=0.7-j0.5	1.694	1.693	1.679
7	L19=0.3-j0.2	1.698	1.698	1.682

2) Partial Loss of Excitation (PLOE)

3) Conditions outlined in examples 2, 4, 6, and 8 have been used to assess the effectiveness of the recommended indices during a PLOE. An excitation system short circuit, an issue with the AVR system, slide rings, or brushes might all result in this scenario. The generator's performance under PLOE is shown in Figs. 15a and 15b, together with the trip-time signals produced by DRPLOEI and DILOEI under conditions of high inductive loading (case 2). But Figs. 16a and 16b show how DILOEI and DRPLOEI operate once more in the context of PLOE conditions, but this time under high capacitive loading (case 6). With a slower rate of decrease, the changes in the generator characteristics are precisely the same as under the TLOE condition (see Figs. 12 and 13). Because there is some interruption to the excitement. Thus, in cases 2 and 6, the trip signal increases somewhat (to 1.719 s for DILOEI and 1.713 s for DRPLOEI, and to 1.702 s for both DILOEI and DRPLOEI). Since the generator's behavior in instances 4 and 8 is consistent with what is shown in Figs. 15 and 16 for cases 2 and 6, the waveforms of the other examples are not included in order to maintain brevity. In conclusion, the trip time signals generated by DILOEI for examples 4 and 8 are 1.715 and 1.712 s, respectively, whereas the comparable values for DRPLOEI are 1.715 and 1.711 s.

Fig. 17. depicts the performance of DRPFLOEI in heavy inductive (case 2) and heavy capacitive loading (case 6) in the PLOE condition. The variation of the key generator values in such a condition follows the same role as the TLOE condition, which was analyzed and illustrated earlier in Fig. 14. But, since the excitation system is not interrupted completely in PLOE, the rate of variations of parameters shows smaller values compared with TLOE. According to the last sub-figure of Fig. 17, DRPFLOEI sends the trip command after 1.689 s and 1.683 s for cases 2 and 6, respectively. Finally, the performance of various introduced indices on the SMIB system under the PLOE condition is summarized in Table IV. Accordingly, in PLOE, DRPFLOEI shows the fastest operation again.

It is worth noting that, in order to demonstrate the satisfactory operation of the DRPFLOEI under both TLOE and PLOE conditions, the graphical simulation results of this index are also provided in Fig. 18 for two more situations. As a result, Fig. 18a depicts the performance of this index under light inductive loading after TLOE (case 3), while Fig. 18b depicts the operation of the same index under light capacitive loading after PLOE (case 8).

TABLE IV
Performance of Different Indices Following Ploe

Case	Loading Type	DILOEI	DRPLOEI	DRPFLOEI
2	L9=0.9+j0.3	1.719	1.713	1.689
4	L2=0.1+j0.2	1.715	1.715	1.696
6	L13=0.7-j0.5	1.702	1.702	1.683
8	L19=0.3-j0.2	1.712	1.711	1.686

4) Stable Power Swing (SPS)

As discussed in [30], one of the main draw-backs of the traditional LOE methods is the mal-operation of them following SPS or OOS. So, the proposed method should block the trip signal during SPS conditions. For this aim, the performance of the mentioned indices versus the SPS condition has been analyzed in various conditions, such as short circuit and load rejection, in a sample TMIB system, and the results are presented in Table V. Accordingly, against the conventional LOE detection method, all the indices have no mal-operation and show reliable performance during SPS. Besides, the 7th scenario of Table V shows a sample of a slowly cleared fault that leads to OOS in the system. Accordingly, all the proposed indices demonstrate suitable performance with no mal-operation during slowly cleared faults.

TABLE V
Performance of Different Indices Following Sps and Its Comparison with Conventional Method

Case	SPS	t_c (ms)	Initial Loading (p.u.)			Performance of different Methods					
						Impedance-based Method			Proposed Indices		
			G1	G2	G3	G1	G2	G3	G1	G2	G3
1	SC on Line 1	230	0.6-j0.3	0.7+j0.2	0.7+j0.4	No Trip	Trip @ 1.772 s	No Trip	No Trip	No Trip	No Trip
2	SC on Line 4	280	0.4-j0.4	0.6-j0.4	0.5-j0.2	Trip @ 1.714 s	Trip @ 2.061 s	No Trip	No Trip	No Trip	No Trip
3	SC on Line 7	350	0.7+j0.3	0.8+j0.4	0.3-j0.4	No Trip	No Trip	Trip @ 2.356 s	No Trip	No Trip	No Trip
4	SC on Line 1	300	0.8+j0.5	0.75+j0.5	0.5+j0.25	No Trip	No Trip	No Trip	No Trip	No Trip	No Trip
5	Load 1&2 Rejection	---	0.8+j0.4	0.8+j0.4	0.8+j0.4	No Trip	No Trip	No Trip	No Trip	No Trip	No Trip
6	Load 3&4 Rejection	---	0.8+j0.4	0.8+j0.4	0.8+j0.4	No Trip	No Trip	No Trip	No Trip	No Trip	No Trip

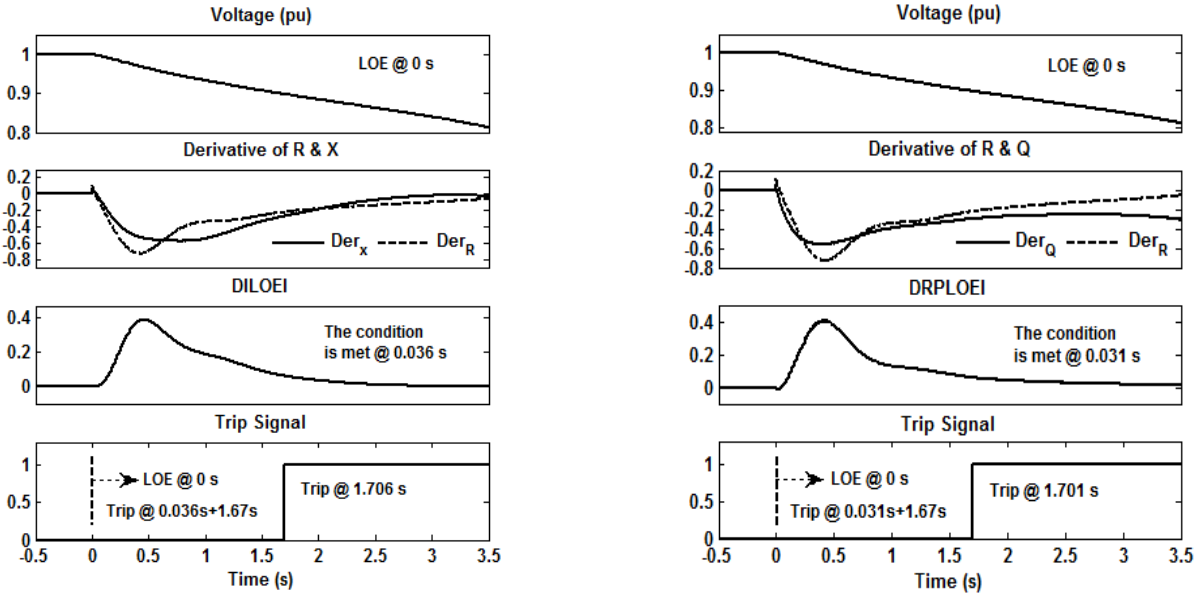

(a) (b)

Fig. 12. The behavior of key parameters and the performance of the proposed method considering (a) DILOEI (b) DRPLOEI in case 1

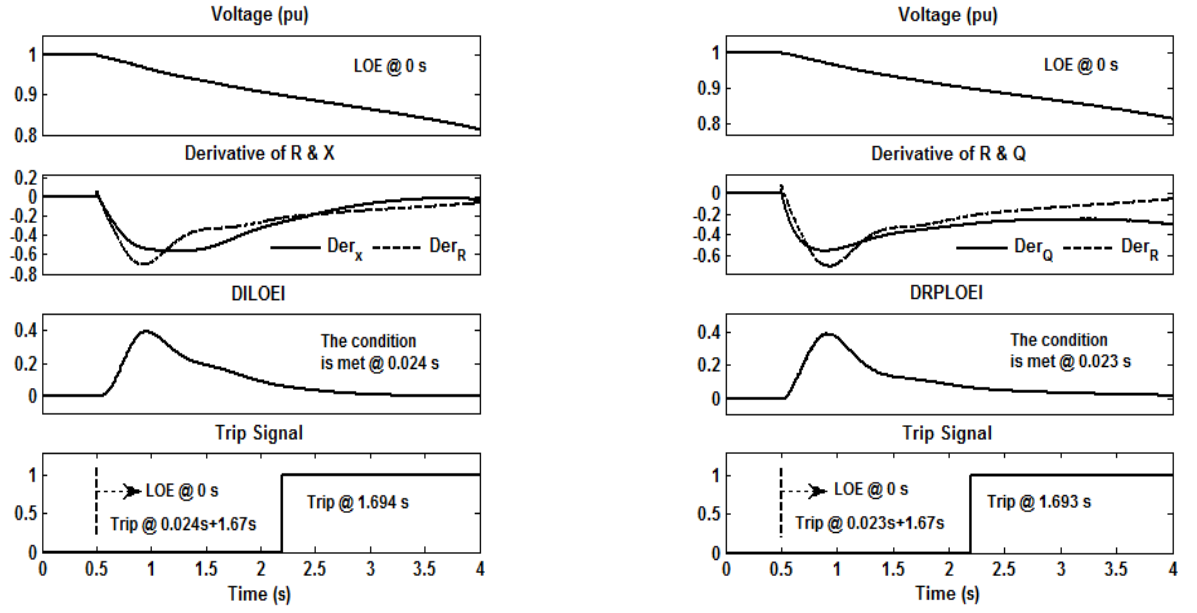

(a) (b)

Fig. 13. The behavior of key parameters and the performance of the proposed method considering (a) DILOEI (b) DRPLOEI in case 5

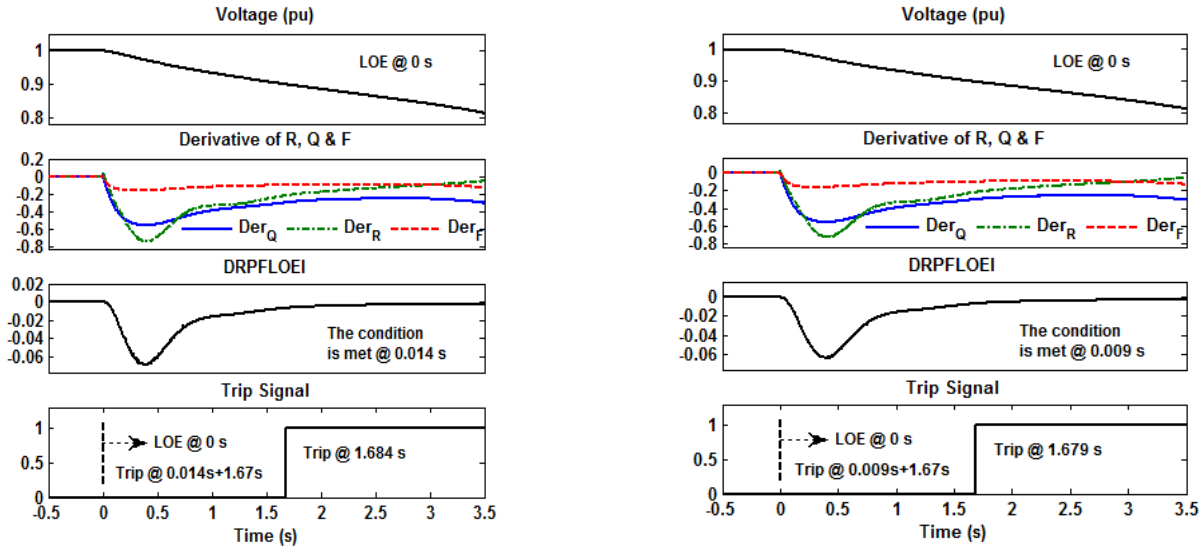

(a) (b)

Fig. 14. The behavior of key parameters and the performance of the proposed method considering DRPFLOEI (a) in case 1 (b) in case 5

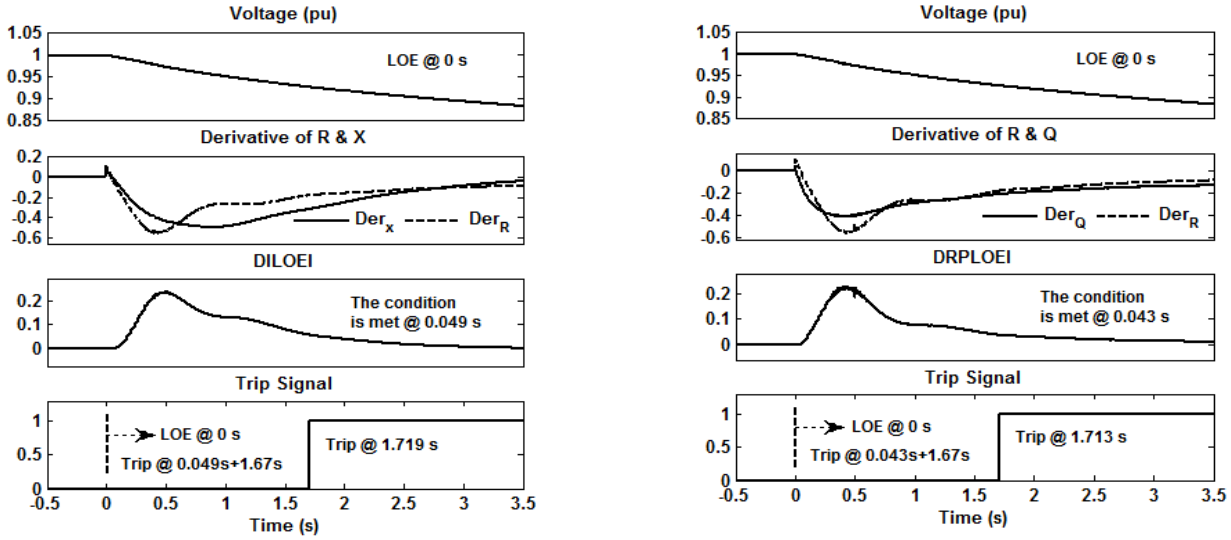

(a) (b)

Fig. 15. The behavior of key parameters and the performance of the proposed method considering (a) DILOEI (b) DRPLOEI in case 2

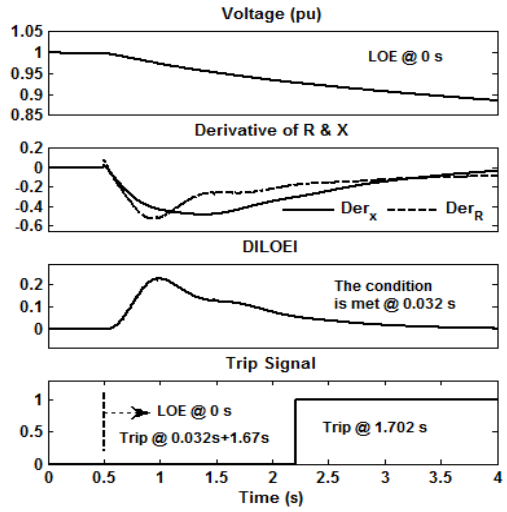

(a)

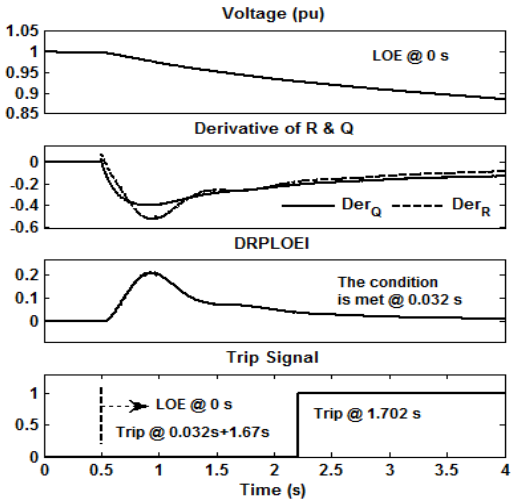

(b)

Fig. 16. The behavior of key parameters and the performance of the proposed method considering (a) DILOEI (b) DRPLOEI in case 6

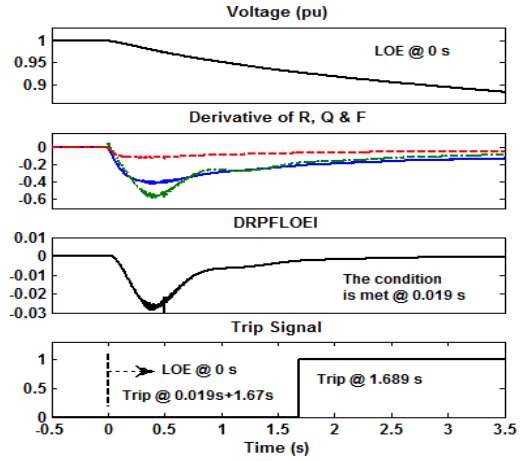

(a)

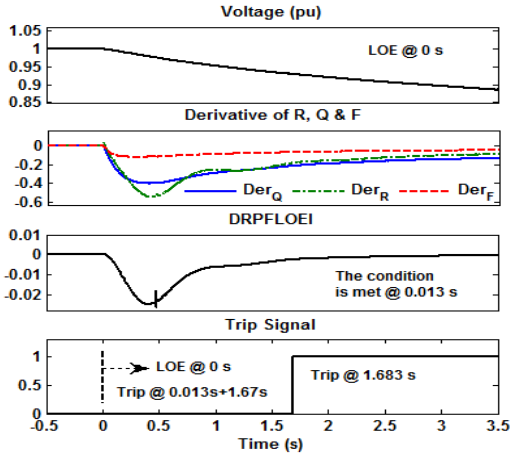

(b)

Fig. 17. The behavior of key parameters and the performance of the proposed method considering DRPFLOEI (a) in case 2 (b) in case 6

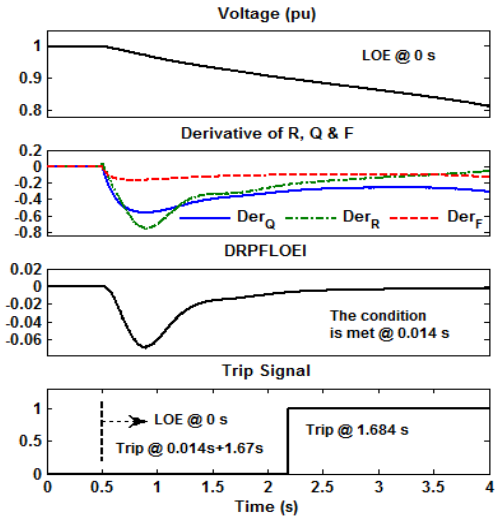

(a)

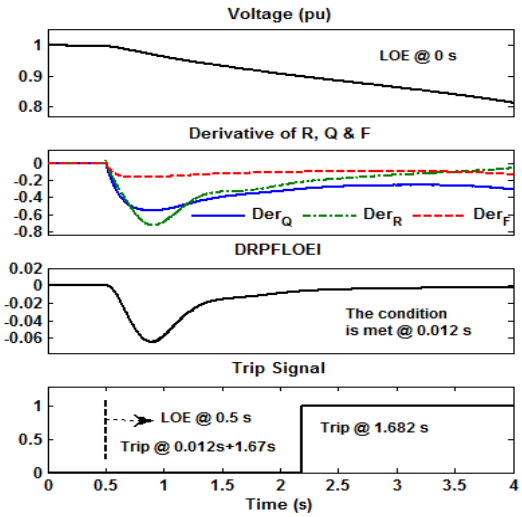

(b)

Fig. 18. The behavior of key parameters and the performance of the proposed method considering DRPFLOEI (a) in case 3 (b) in case 8

TABLE VI
Characteristics of Various Detection Methods Along with Comparison with the Proposed Technique

Method	Ref.	Characteristics
Impedance-Based	[6-9]	Low Speed, Low Accuracy, Dependent on load, generator and network conditions
Reactance and Admittance-Based	[10]	High Speed, Dependent on load, generator and network conditions
ANN and Support Vector Machine	[11, 13-16]	High Speed, Low reliability against unexpected faults, using many parameters of generator and network
Fuzzy Logic	[12]	Low Speed, Low Accuracy for leading loads, Dependent on load, generator and network conditions
Based on Q/δ and $V/Q/\delta$	[18, 19]	High Speed, mal-operation during SPS, Lack of suitable theory in determining some parameters and operating method
Resistance-Based	[20]	Low Speed, Dependent on load, generator and network conditions
Flux-based	[34, 36, 37]	High Speed, High Accuracy, Difficulty in measuring flux, Dependent on load, generator and network conditions
Based on Reactive Power	[24]	High Speed, mal-operation against TLOE, Dependent on load, generator and network conditions
Based on Internal Voltage	[25, 26]	Moderate Speed, capable theory in determining parameters, Dependent on load, generator and network conditions
Based on V/Q	[33]	High Speed, Low Accuracy during SPS, Lack of suitable theory in determining some parameters
Based on IEEE C37.102	[29]	Moderate Speed, Dependent on the network conditions, lower accuracy during SPS.
Z-Based Considering SCV Effect	[30]	Moderate Speed, Dependent on load, generator and network conditions, lower accuracy during SPS
Based on Q Change Strategy	[27]	Moderate Speed, Dependent on load, generator and network conditions
Based on Freq. Decomposition of P, Q & V	[32]	High Speed, Lower Accuracy during SPS
Proposed Technique		Highest Speed, High Accuracy and reliability in discriminating SPS and OOS from LOE, capable theory in determining parameters, Non-dependent on load, generator and network conditions, Setting-free

V. COMPARATIVE ANALYSIS

This section first compares the advantages and disadvantages of various recent LOE protection methods with the proposed technique in Table VI. Accordingly, the recent methods have modified the conventional schemes, but they still suffer from some problems. However, the introduced algorithm of this study could effectively overcome the expected mal-operation of other methods.

Besides, in order to show the satisfactory performance of the proposed technique, the operations of all the indices for a sample 390 MVA generator in heavy capacitive loading have been compared with various available techniques, including:

1) Positive Offset
2) Berdy
3) LOE detection method on the basis of fuzzy inference mechanism (LOE-FIM)
4) LOE detection method on the basis of flux method (LOE-FBM)
5) LOE protection based on flux method combined with negative sequence current (LOE-FVNSC)
6) LOE Based on IEEE C37.102
7) Z-Based Considering SCV Effect Removal
8) LOE-RPI (Reactive Power Index)
9) Freq. Decomposition of P, Q & V
10) LOE Based on V, Q & δ

The final results are summarized in Table VII.

As expressed earlier and according to Table VII, the proposed indices have the best operation among all other method and also DRPFLOEI with 1.679 s of delay has the fastest performance among all the indices.

TABLE VII
Performance Comparison of Different LOE Detection Methods

The Applied Method	Ref. No.	Trip Time (s)
Positive offset	[7, 8]	11.2
Berdy	[9]	10.4
LOE-FIM (Fuzzy Interference Mechanism)	[12]	9.1
LOE-FVNSC (Flux Versus Neg. Seq. Current)	[40]	3.1
LOE-FBM (Flux-Based Method)	[36, 37]	3.1
LOE Based on IEEE C37.102	[29]	5.123
Z-Based Considering SCV Effect Removal	[30]	3.68
LOE-RPI (Reactive Power Index)	[27]	3.520
Freq. Decomposition of *P, Q & V*	[32]	2
LOE Based on *V, Q & δ*	[18]	1.831
Proposed Method applying DILOEI		1.694
Proposed Method applying DRPLOEI		1.693
Proposed Method applying DRPFLOEI		1.679

VI. CONCLUSION

This contribution introduces three different combined indices, including DILOEI, DRPLOEI, and DRPLOEI, on the basis of the derivative of the generator parameters such as R, X, Q and φ for LOE detection. The performance of all indices has been evaluated considering various scenarios and extensive simulations, and consequently, the DRPFLOEI is found to be the best index. Besides, DRPFLOEI expressed the fastest and also the most reliable operation among all usual methods and also other recent studies. In fact, in addition to the higher speed of operation, all the proposed indices are capable of discriminating LOE from SPS, which can effectively prevent the mal-operation of the relay. The suggested technique is almost independent from the value and type of loading, the configuration of the power network, and also the generator size.

APPENDIX

TABLE A1
Data for Smib Network [34, 41, 42]

With steam turbine	With hydraulic turbine
S=600 MVA, f=60 Hz, V=22kv	S=390 MVA, f=60 Hz, V=24kv
X_d=1.65 pu, X'_d(pu)=0.25 pu	X_d=1.35 pu, X'_d(pu)=0.296 pu
X''_d=0.2 pu, X_q=1.59 pu	X''_d=0.252 pu, X_q=0.474 pu
X'_q=0.46 pu, X''_q=0.2 pu	X''_q=0.243 pu, X_1=0.18 pu
X_1=0.14 pu, T'_{do}=4.5 s	T'_{do}=5 s, T''_{d0}=0.1 s
T''_{d0}=0.04 s, T'_{qo}=0.67 s	T''_{qo}=0.09 s, R_s=0.0028 pu
T''_{qo}=0.09 s, R_s=0.0045 pu	
Inertia constant (H)= 0.8788 s	Inertia constant (H)= 5.5 s
Transformer= j0.15 pu, Transmission Line= j0.5 pu	

TABLE A2
Data for Tmib Network [34, 41, 42]

Generators
G1: S= 80 MVA, V= 13.8 kv, H= 3.5 s
G2: S= 390 MVA, V= 13.8 kv, H= 5.5 s
G3: S= 500 MVA, V= 13.8 kv, H= 4 s
Transmission lines
L1: Z= 0.048+ j0.48 Ω, **L2:** Z= 0.00576+j 0.573 Ω
L3: Z= 0.0288+0.288 Ω, **L4:** Z= 0.0576+j 0.576 Ω
L5: Z= 0.0142+j 0.142 Ω, **L6:** Z= 0.00192+j 0.192 Ω
L7: Z= j 0.0957 Ω

VII. REFERENCES

[1] IEEE Guide for AC Generator Protection, IEEE Standard. C37.102, 2006.

[2] Z. Yulan, X. Yong 'Operation statistics and analysis of relay protection and automatic devices of Chinese power systems in 1995', Power Syst. Technol., 1996, 20, (12), pp. 57–61.

[3] P. Kundur, 'Power system stability and control' (McGraw-Hill, New York, 1994).

[4] North Electric Reliability Corporation (NERC)-System Protection and Control Subcommittee: 'Power plant and transmission system protection coordination', Technical Reference Document, 2010, pp. 72–81

[5] H. Yaghobi, 'Impact of static synchronous compensator on flux-based synchronous generator loss of excitation protection', IET Gen. Trans. and Dist., 9(9), pp. 874-883, (2015).

[6] D. Reimert, 'Protective relaying for power generation systems' (Boca Raton, CRC Press, 2006)

[7] C.R. Mason, 'A new loss-of-excitation relay for synchronous generators', Transactions of the American Institute of Electrical Engineers, 68(2), pp. 1240–1245, (1949).

[8] R.L. Tremaine and J.L. Blackburn, 'Loss-of-field protection for synchronous machines', Journal of Electrical Engineering, 73(11), pp. 1008-1008, (1954).

[9] J. Berdy, , 'Loss-of-excitation protection for synchronous generators', IEEE Transactions on Power Apparatus and Systems, 94(5), pp. 1457–1463, (1975).

[10] H.J. Herrman, A. Smit, 'Increased sensitivity of loss of field protection based on admittance measurement', In: Western protective relay conference, Washington DC, USA, October 2009, pp. 1–15.

[11] A.M. Sharaf, T.T. Lie, 'ANN based pattern classification of synchronous generator stability and loss of excitation', IEEE Trans.Energy Convers., 9(4), pp. 753–759, (1994).

[12] A.P. Morais, C. G. Mariotto 'An innovative loss-of excitation protection based on the fuzzy inference mechanism', IEEE Trans Power Deliv., 25(4), pp. 2197–2204, (2010).

[13] S.R. Samantaray and P.K. Dash, 'Transmission line distance relaying using machine intelligence technique', IET Gener. Transm. Distrib., 2(1), pp. 53–61, (2008).

[14] N. Chothani, B. Bhalja, U. Parikh, 'New support vector machine-based digital relaying scheme for discrimination between power swing and fault', IET Gener., Transm. Distrib., 8(1), pp. 17–25, (2014).

[15] B. Bhalja, N. Chothani, U. Parikh, 'Development of a new bus zone identification algorithm using support vector machine', IET Gener., Transm. Distrib., 6(7), pp. 710–718, (2012).

[16] L.M. Saini, S.K. Aggarwal, A. Kumar, 'Parameter optimization using genetic algorithm for support vector machine-based price-forecasting model in National electricity market', IET Gener., Transm. Distrib., 4(1), pp. 36–49, (2010).

[17] M. Rasoulpour; T. Amraee and A. Sedigh, 'A Relay Logic for Total and Partial Loss of Excitation Protection in Synchronous Generators', IEEE Transactions on Power Delivery, 35(3), pp. 1432-1442, (2020).

[18] A. Hasani and F. Haghjoo, 'A Secure and Setting-Free Technique to Detect Loss of Field in Synchronous Generators', IEEE Trans. Energy Conv., 32(4), pp. 1512-1522, (2017).

[19] A. Hasani; F. Haghjoo, 'Fast and secure detection technique for loss of field occurrence in synchronous generators', IET Electric power applications, 11(4), pp. 567-577, (2017).

[20] B. Mahamedi; J. G. Zhu; and S. M. Hashemi, 'A setting-free approach to detecting loss of excitation in synchronous generators', IEEE Transactions On Power Delivery, 31(5), pp. 2270-2278, (2016).

[21] H. Yaghobi, 'A new adaptive impedance-based LOE protection of synchronous generator in the presence of STATCOM', IEEE Transactions on Power Delivery, 32(6), pp. 2489-2499, (2017).

[22] M. Ostojic, M. Djuric, 'The algorithm for the detection of loss of excitation of synchronous generators based on a digital-phase comparator', Electrical Engineering Journal, 100, pp. 1287-1296, (2018).

[23] A. Hasani; F. Haghjoo and C. L. Bak, 'A Current-Based Differential Technique to Detect Loss of Field in Synchronous Generators', IEEE Transactions on Power Delivery, 35(2), pp. 514-522, (2020).

[24] N. Noroozi; Y. Alinejad-Beromi and H. Yaghobi, 'Fast approach to detect generator loss of excitation based on reactive power variation,' IET Generation, Transmission & Distribution, 13(4), pp. 453-460, (2019).

[25] M. Abedini, M. Sanaye-Pasand and M. Davarpanah, 'An Analytical Approach to Detect Generator Loss of Excitation Based on Internal Voltage Calculation', IEEE Transactions On Power Delivery, 32 (5), pp. 2329-2338, (2017).

[26] A. Rostami, N. Rezaei, "An Improved Setting-Free Scheme for Fast and Reliable Detection of Complete and Partial Loss-of-Excitation", IEEE Systems Journal, 17(1), pp. 860 – 868, (2023).

[27] A. Rostami, N. Rezaei, "A Novel Loss-of-Excitation Protection Strategy Based on Reactive Power Increment of Synchronous Generators", IEEE Transactions on Power Delivery, 36(6), pp. 3733 – 3742, (2021).

[28] A. Rostami, N. Rezaei, A. Jalilian; B. Naderi, et al., "Load Angle Based Loss of Excitation Protection Scheme for Parallel Connected Synchronous Generators", IEEE Transactions on Industry Applications, 58(6), pp. 6960 - 6969, (2022).

[29] A. Hasani, F. Haghjoo, C. L. Bak and F. F. da Silva, "STATCOM Impacts on Synchronous Generator LOE Protection: A Realistic Study Based on IEEE Standard C37. 102", IEEE Transactions on Industry Applications, 57(2), pp. 1255 – 1264, (2021).

[30] F.C. Neves a, A.L.M. Coelho and I.P. Faria., "A testbed for assessing the impact of static var compensator on loss of excitation protection of synchronous generators", Electric Power Systems Research, 201(1), pp. 1 - 11, (2021).

[31] F. A. de Oliveira, E. M. dos Santos, C. D. L. da Silva; E. D. Kilian, et al, "Synchronous Generator Loss of Excitation Detection Technique Based on Waveforms Envelopes Analysis", IEEE PES GTD Latin America, La Paz, Bolivia, 20-22 October 2022, INSPEC No. 22622992.

[32] M. Rasoulpour, T. Amraee, and A. Khaki Sedigh, "A Relay Logic for Total and Partial Loss of Excitation Protection in Synchronous Generators", IEEE Transactions on Power Delivery, 35(3), pp. 1432 - 1442, (2020).

[33] Mahdi Amini; Mahdi Davarpanah and Majid Sanaye-Pasand, 'A novel approach to detect the synchronous generator loss of excitation', IEEE Transactions on Power Delivery, 30(3), pp. 1429-1438, (2015).

[34] H. Yaghobi, 'Fast discrimination of stable power swing with synchronous generator loss of excitation', IET Gen. Trans. and Dist., 10(7), pp. 1682-1690, (2016).

[35] H. Yaghobi, 'Out-of-step protection of generator using analysis of angular velocity and acceleration data measured from magnetic flux', Electric Power Systems Research, 132, pp. 9–21, (2016).

[36] Hamid Yaghobi; and Hashem Mortazavi, 'A novel method to prevent incorrect operation of synchronous generator loss of excitation relay during and after different external faults', European Transactions on Electrical Power, 25(9), pp. 1717-1735, (2014).

[37] H. Yaghobi, H. Mortazavi, K. Ansari, et al., "Study on application of flux linkage of synchronous generator for loss of excitation protection, European Transactions on Electrical Power, 23(6), pp. 802-817, (2013).

[38] H. Yaghobi, Fast predictive technique for reverse power detection in synchronous generator", IET Electric Power Applications, 12(4), pp. 508-517, 2018.

[39] M. Elsamahy, S. O. Farihed and T. Sidhu, 'Impact of midpoint STATCOM on generator LOE protection', IEEE Transactions on Power Delivery, 29(2), pp. 724-732, (2014).

[40] H. Yaghobi, 'Impact of static synchronous compensator on flux-based synchronous generator loss of excitation protection', IET Gener. Transm. Distrib., 9(9), pp. 874–883, (2015).

[41] M. Samami and M. Niaz Azari., "Novel fast and secure approach for reverse power protection in synchronous generators" IET Electric Power Applications, 13(12), pp. 2128-2138, (2019).

[42] M. Samami and M. Niaz Azari., "Fast and Secure Angular-Based Detection Algorithm for Reverse Power Occurrence in Synchronous Generators", Scientia Iranica, doi: 10.24200/sci.2021.58407.5711, (2021).